Supplement of The Cryosphere, 20, 2469–2484, 2026
https://doi.org/10.5194/tc-20-2469-2026-supplement

The Cryosphere Open Access EGU

Supplement of

Impact of spatial resolution on large-scale ice cover modelling of mountainous regions

Helen Werner et al.

Correspondence to: Helen Werner (helen.werner@gfz.de)

S1 Additional maps

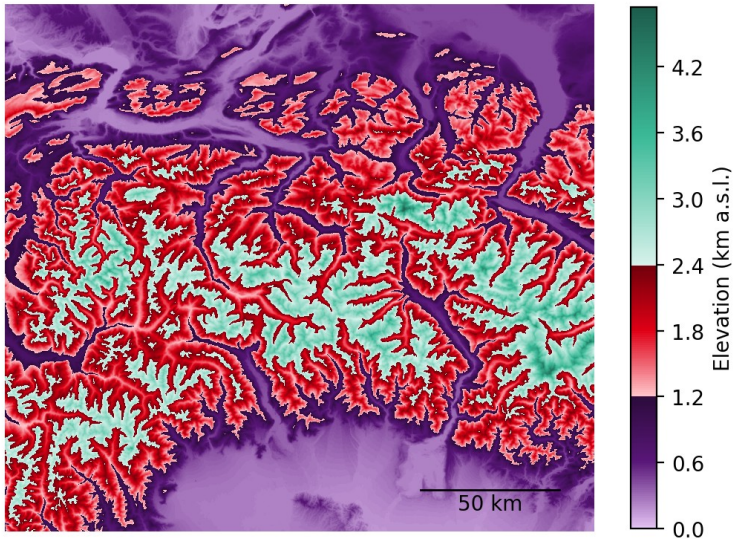

Figure S1 Map of our model region showing our defined elevation bands for low (0–1200 m a.s.l., purple), mid (1200–2400 m a.s.l., red), and high altitudes (<2400 m a.s.l., green).

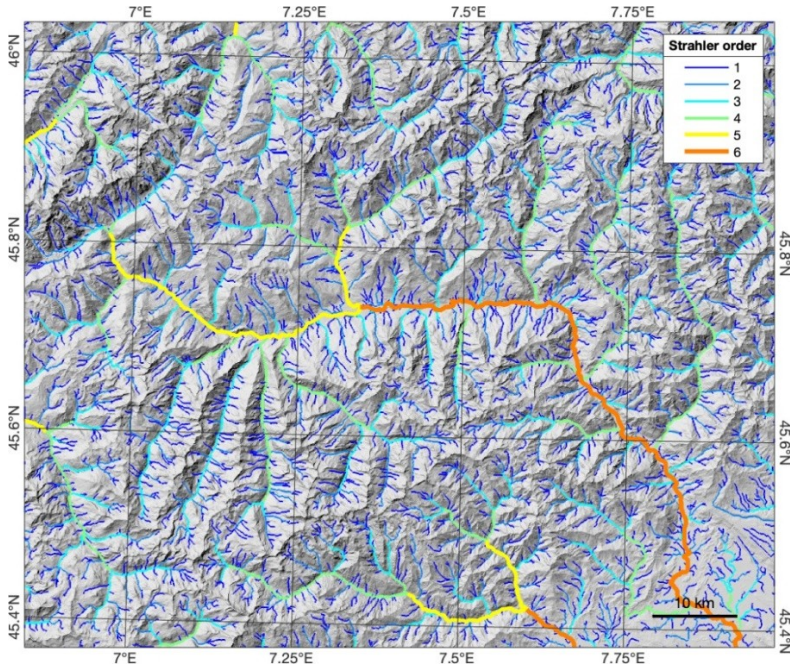

Figure S2 Map of the Aosta Valley in Italy with colour-coded streams according to their Strahler stream order (Strahler, 1957). The Strahler order defines the stream size based on a hierarchy of tributary streams. Streams of order 1 (dark blue) are the smallest streams without any tributaries. As the stream order increases, the streams and associated valleys have more branches upstream and their sizes increase. The largest streams in this area are of Strahler order 6 (orange).

S2 Ice field conditions at full glaciation

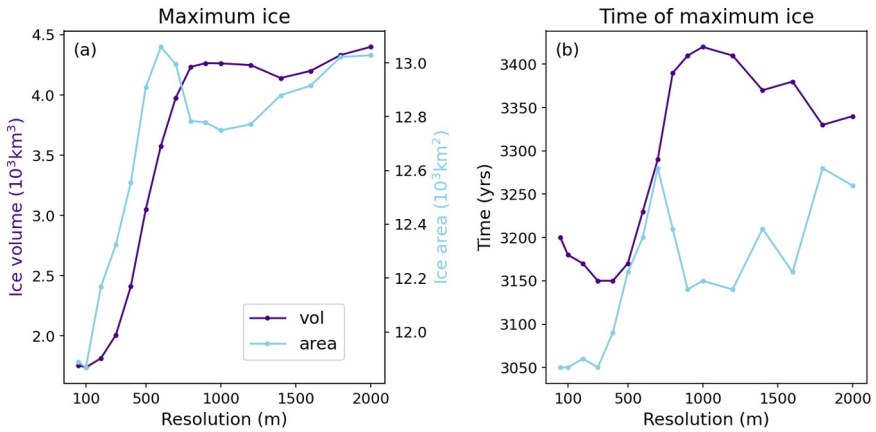

Figure S3 (a) Maximum ice volume (purple) and area (blue), (b) time of maximum ice volume (purple) and area (blue) for simulations at all resolutions.

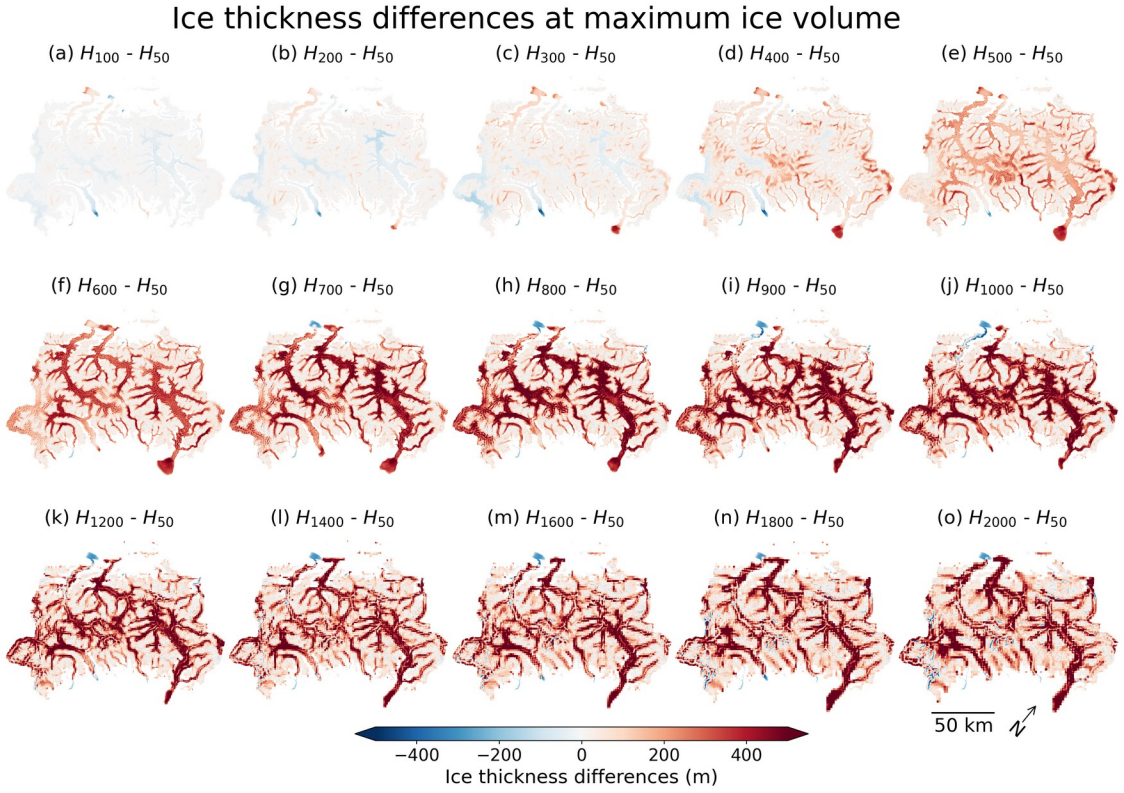

Figure S5 Ice thickness differences $\Delta H = H_r$-H_{50} at maximum ice volume between models at resolution r and the 50 m reference run. This figure is an expanded version of Fig. 5 in the main text.

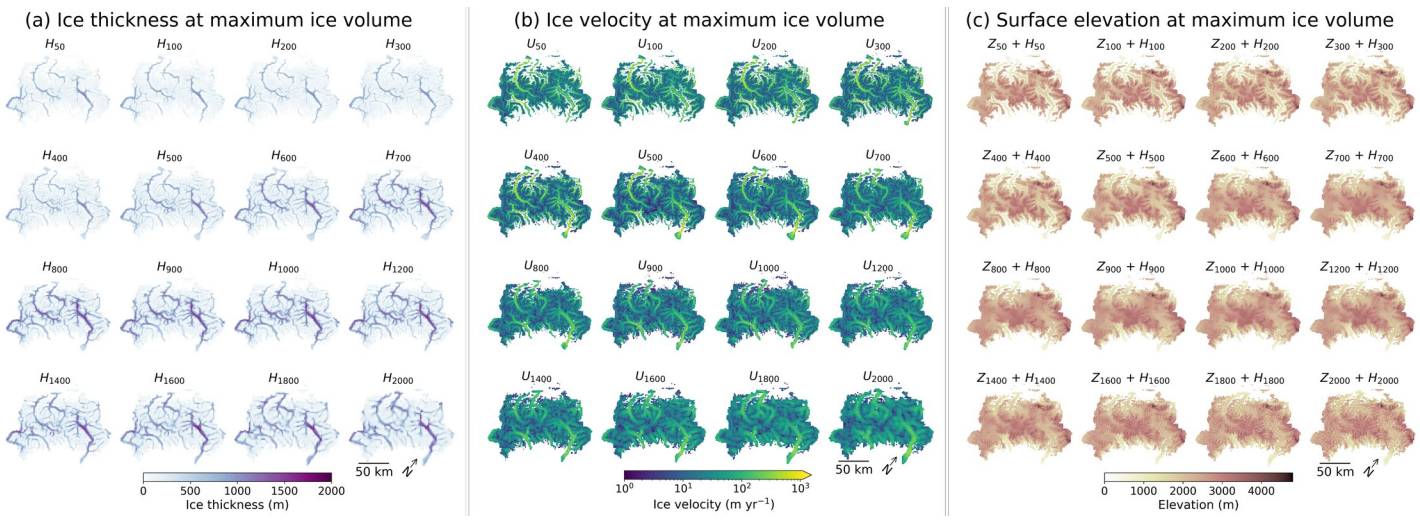

Figure S4 (a) Ice thickness H_r, (b) depth-averaged ice velocity U_r, (c) surface elevation (bedrock elevation Z_r plus ice thickness H_r) at maximum ice volume for simulations at resolution r.

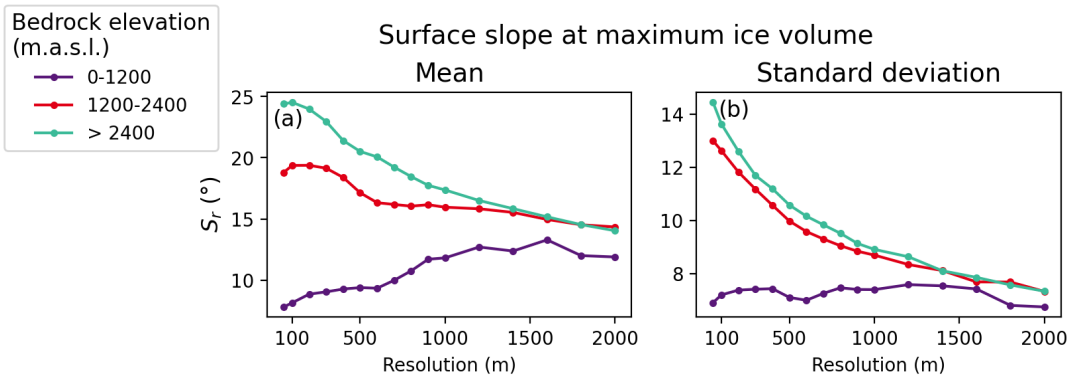

Figure S6 (a) Mean and (b) standard deviation of slope angle of surface elevation (bedrock elevation and ice thickness) at full glaciation across the glaciated area at low (0–1200 m a.s.l.), mid (1200–2400 m a.s.l.), and high (>2400 m a.s.l.) altitudes.

S3 Simulations using slower temperature forcing

The following figure shows model outputs from simulations using a fast temperature forcing with 4 °C temperature change per 1,000 years shown in Figs. 3-7 in the main text and slow temperature forcing with 2 °C temperature change per 1,000 years. In model years, the cooling phase spans 1000–3000 years under fast and 1000–5000 years under slow temperature forcing, and the warming phase spans 3000–5000 years under fast and 5000–9000 years under fast temperature forcing. For a more detailed description of the applied temperature forcings we refer to section 2.2 in the main text.

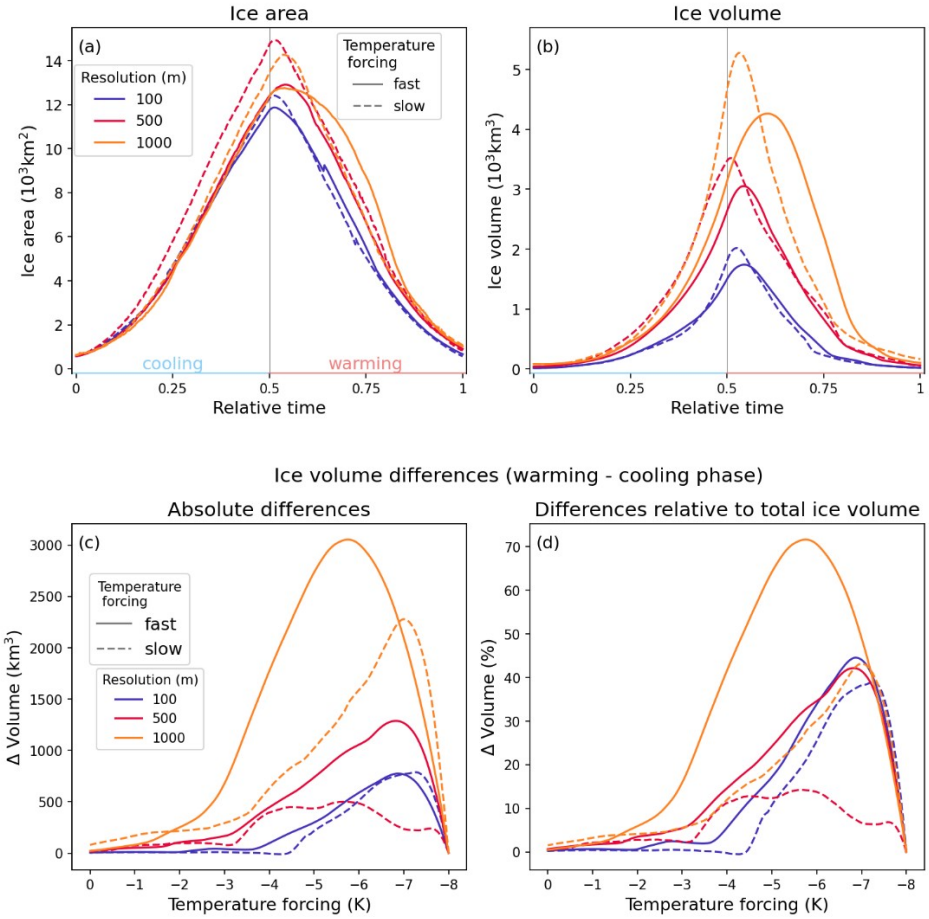

Figure S7 Ice volume and area under fast (solid line) and slow (dashed line) temperature forcing at 100 (blue), 500 (red), and 1000 m (orange) resolution. (a) Ice area, (b) ice volume over relative time. Relative time on the x-axis ranges from 0 (start of cooling phase with a temperature forcing of 0 K) to 1 (end of cooling phase with a temperature forcing of 0 K). At 0.5, half of the simulation is reached, where temperature forcing is strongest at -8 K and the warming phase begins. (c) Absolute and (d) relative differences of ice volume at times with the same temperature forcing value during the warming and cooling phases (warming minus cooling phase). Panel (a) is similar to Fig. 3c, and differences in (d) are relative to the total ice volume.

S4 Experiments with smoothed DEMs

The following two figure show input and outputs from additional experiments based on a smoothed topography. The smoothed topography is obtained through the following process: We took the DEM of our model domain at 2 km resolution, which was created from the fine resolution DEM using cubic resampling. Therefore, the 2 km DEM is rather smooth with less topographic detail. We then proceeded to interpolate the 2 km DEM back to finer resolutions, again using cubic convolution. The mean slope angle of the original DEM is 21.5°, and of the smoothed DEM is 11.5°.

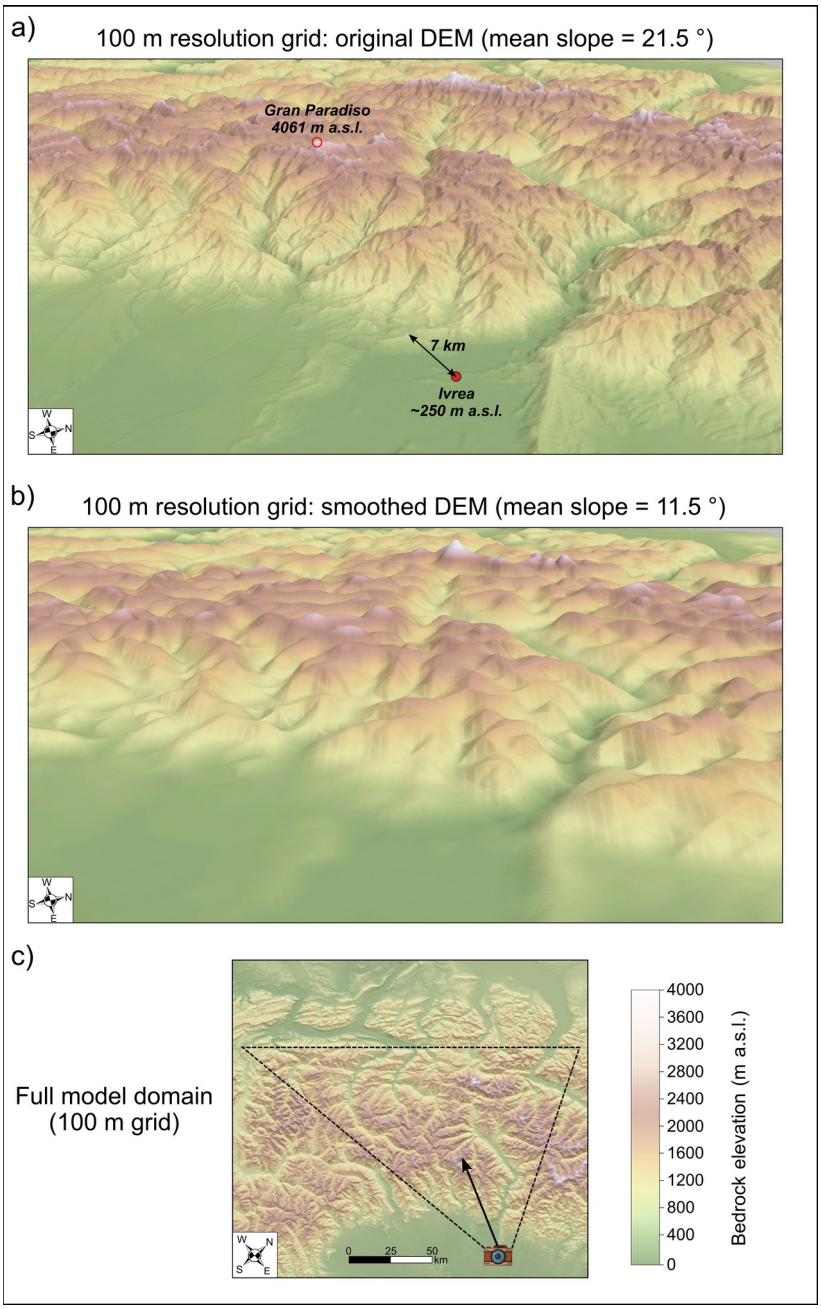

Figure S8 Comparison of (a) original and (b) smoothed DEM, both at 100 m resolution. The smoothed DEM is based on the 2000-m DEM using cubic resampling at 100 m. The perspective of (a) and (b) inside the model domain (original 100-m DEM) is shown in (c). All panels were produced using ArcGIS Pro 3.2.2 (Esri).

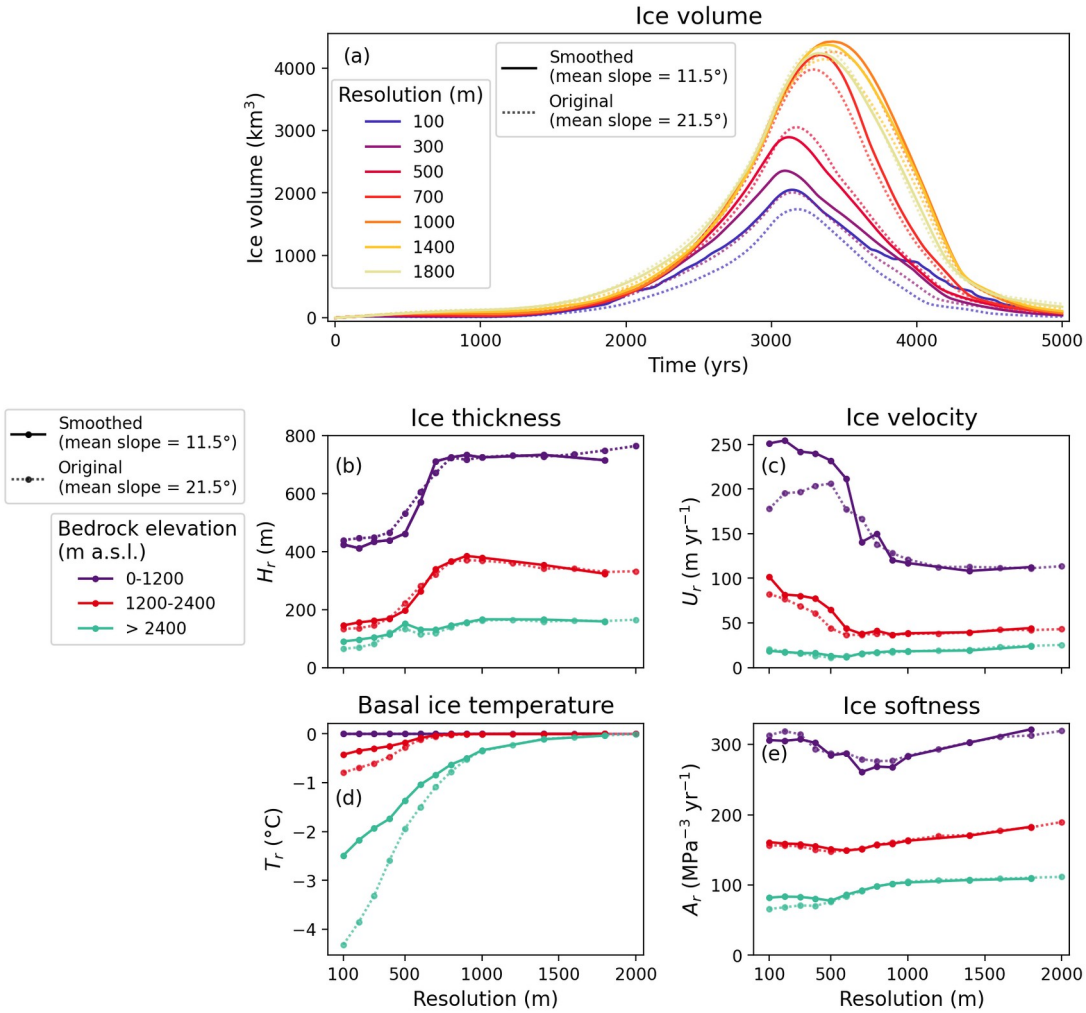

Figure S9 Comparison of simulations based smoothed DEMs to simulations based on the original DEMs. (a) Temporal evolution of ice volume, at 100, 300, 500, 700, 1000, 1400, 1800 m resolutions. (b)–(e) Model output variables at full glaciation averaged over glaciated area at different resolutions *r*, distinguished between low (0–1200 m a.s.l.), mid (1200–2400 m a.s.l.), and high (>2400 m a.s.l.) bedrock altitudes (similar to Fig. 7 in the main text): (b) Ice thickness H_r, (c) depth-averaged ice velocity U_r, (d) basal ice temperature T_r, (f) depth-averaged Arrhenius factor A_r. In all subplots, solid lines correspond to results based on the smoothed DEMs, and dashed lines correspond to results based on original DEMs.

S5 Model parameters and climate input

Table S1 IGM model parameters that are based on Leger et al. 2025's ensemble best-scoring simulation (simulation 37).

IGM module / parameter name	Description	System component	Value	Unit
Surface mass balance				
smb_accpdd_update_freq	Frequency at which the Surface Mass Balance (SMB) is updated	Surface mass balance	1.0	yr
accpdd_refreeze_factor	Positive Degree Day refreezing factor	Surface mass balance	0.6156090086419556	n/a
smb_accpdd_thr_temp_snow	Threshold temperature for solid precipitation	Surface mass balance	0.0	°C
smb_accpdd_thr_temp_rain	Threshold temperature for liquid precipitation	Surface mass balance	2.0	°C
smb_accpdd_melt_factor_snow	Positive Degree Day melt rate for snow	Surface mass balance	1.20409532638	m *we* °C^{-1} yr^{-1}
smb_accpdd_melt_factor_ice	Positive Degree Day melt rate for ice	Surface mass balance	2.8262694332550296	m *we* °C^{-1} yr^{-1}
smb_accpdd_shift_hydro_year	This serves to start Oct 1 the acc/melt computation	Surface mass balance	0.75	yr
smb_accpdd_ice_density	Density of ice for conversion of SMB into ice equivalent	Surface mass balance	910.0	kg m^{-3}
smb_accpdd_wat_density	Density of water	Surface mass balance	1000.0	kg m^{-3}
Ice flow				
filo_enhancement_factor	Flow law enhancement factor	Ice flow	1.3885266806845515	n/a

IGM module / parameter name	Description	System component	Value	Unit
iflo_regu_glen	Regularisation parameter for Glen's flow law	Ice flow	0.0	n/a
iflo_regu_weertmann	Regularisation parameter for Weertman's sliding law	Basal sliding	10^{-10}	n/a
iflo_exp_glen	Glen's flow law exponent	Ice flow	3.0	n/a
iflo_exp_weertman	Weertman's law exponent	Basal sliding	4.0	n/a
iflo_gravity_cst	Acceleration due to gravity of a free falling object	Ice flow	9.81	m s^{-2}
iflo_ice_density	Density of ice	Ice flow	910.0	kg m^{-3}
iflo_Nz	Number of grid points for the vertical discretisation	Ice flow	10.0	n/a
iflo_vert_spacing	Discretisation density to get more points towards glacier bed than surface	Ice flow	4.0	n/a
iflo_thr_ice_thk	Threshold ice thickness for computing strain rate	Ice flow	0.1	m
iflo_dim_arrhenius	Dimension of the Arrhenius factor (horizontal 2D or 3D)	Ice flow	3.0	n/a
iflo_retrain_emulator_freq	Frequency at which the emulator is retrained, 0 means never, 1 means every time step	Neural network	2.0 (50, 100 m res.)*, 7.0 (else)	time step
iflo_retrain_emulator_lr	Learning rate for the retraining of the emulator	Neural network	10^{-5}	n/a
iflo_retrain_emulator_nbit	Number of iterations at each time step for retraining the emulator	Neural network	1.0	iterations
iflo_force_max_velbar	Artificially upper-bound of ice velocities	Ice flow	3000.0	m yr^{-1}
iflo_network	Type of network, it can be cnn or unet	Neural network	"cnn"	n/a
iflo_nb_layers	Number of layers in the Convolutional Neural Network (CNN)	Neural network	16.0	n/a
iflo_nb_blocks	Number of block layer in the U-net	Neural network	4	n/a
iflo_nb_out_filter	Number of output filters in the CNN	Neural network	32.0	n/a
iflo_conv_ker_size	Size of the convolution kernel	Neural network	3.0	n/a
iflo_dropout_rate	Dropout rate in the CNN	Neural network	0	n/a
iflo_min_sr	Minimum strain rate	Ice flow	10^{-5}	yr^{-1}
iflo_max_sr	Maximum strain rate	Ice flow	1.0	yr^{-1}
thk_slope_type	Slope limiter for the ice thickness equation (godunov or superbee)	Ice flow	"superbee"	n/a
vflo_method	Method to retrieve vertical velocities (kinematic, incompressibility)	Ice flow	"incompressibility"	n/a
Time				
time_start	Simulation start	Time	0.0	yr
time_end	Simulation end	Time	5000.0 (9000.0 with slow temperature forcing)	yr
time_save	Save output frequency	Time	10.0	yr
time_cfl	CFL number for the stability of the mass conservation scheme	Time	0.3	
time_stp_max	Maximum time step allowed, used only with slow ice	Time	10.0	yr
Enthalpy				
enth_water_density	Density of water	Enthalpy	1000.0	kg m^{-3}
enth_spy	Number of seconds in a year	Enthalpy	31556926.0	seconds
enth_ki	Conductivity of cold ice	Enthalpy	2.1	W m^{-1} K^{-1}

IGM module / parameter name	Description	System component	Value	Unit
ent_ci	Specific heat capacity of ice	Enthalpy	2009.0	W s kg^{-1} K^{-1}
enth_Lh	Latent heat of fusion	Enthalpy	334000.0	W s kg^{-1}
ent_KtdivKc	Ratio of temperate versus cold ice diffusivity	Enthalpy	0.1	n/a
enth_claus_clape	Clausius-Clapeyron constant	Enthalpy	7.9×10^{-8}	K Pa^{-1}
enth_melt_temp	Melting point at standard pressure	Enthalpy	273.15	K
enth_ref_temp	Reference temperature	Enthalpy	223.15	K
enth_till_friction_angle_bed_min	Lower bed elevation threshold for yield stress	Yield stress	-444.8608285471192	m a.s.l.
enth_till_friction_angle_bed_max	Upper bed elevation threshold for yield stress	Yield stress	2982.864772500515	m a.s.l.
ent_till_friction_angle_phi_min	Minimum till friction angle in bed-elevation dependent scheme	Yield stress	15.0	°
enth_till_friction_angle_phi_max	Maximum till friction angle in bed-elevation dependent scheme	Yield stress	50.0	°
enth_uthreshold	Pseudo-plastic sliding law U threshold	Sliding	1244.8467164648443	m yr^{-1}
enth_drain_rate	Water draining rate	Yield stress	0.001	mm yr^{-1}
enth_till_wat_max	Maximum water till thickness	Yield stress	2.0	m
enth_default_bheatflx	Geothermal heat flux	Basal melt	0.065	W m^{-2}
temperature_offset_air_to_ice	Surface air-to-ice temperature offset	Enthalpy	2.9022389684294243	°C
enth_tauc_min	Lower caping bound for yield stress	Yield stress	10000.0	Pa
enth_tauc_max	Upper caping bound for yield stress	Yield stress	1 0000000000.0	Pa
Avalanche				
avalanche_update_freq	Update frequency of the avalanche module	Avalanche	5.0	yr
avalanche_angleOfRepose	Angle of repose. For bed slopes above this, ice “avalanches”	Avalanche	45.0	°
Gflex				
gflex_update_freq	Update frequency of the gFlex GIA module	Glacial isostatic adjustment	50.0	yr
gflex_default_Te	Lithospheric effective elastic thickness	Glacial isostatic adjustment	45556.89245060796	m
gflex_dx	Spatial grid resolution of the gFlex GIA module	Glacial isostatic adjustment	2000.0	m

* The retraining frequency is 7.0 for simulations at resolutions of 200 m and coarser (as in Leger et al., 2025), and 2.0 for the highest-resolution simulations at 50 and 100 m resolution.

Table S2 Initial monthly temperature and precipitation (similar to present-day). The data is derived from climate data averaged over 1981–2010 from a weather station in Modane, France, located at 1228 m a.s.l. within the model domain (Météo France, 2022), precipitation values were uniformly multiplied by 1.6. Throughout the model runs, temperature values were modified by the temperature forcing.

Month	**Temperature** (°C)	**Precipitation** (kg m^{-2} yr^{-1} *we*)
January	-1.4	1040.610
February	-0.4	1150.180
March	3.3	876.608
April	6.4	974.000
May	11.4	1065.120
June	14.4	1129.840
July	16.9	788.000
August	16.6	1046.270
September	12.8	1040.240
October	8.7	1246.100
November	2.2	1217.500
December	-0.8	1074.540